Assessment of the influence of discontinuity constitutive models for modelling fractured rock masses

Cammarata, G.; Bui, T.A.; Brasile, S.; Skordilis, V.; Brinkgreve, R.

Publication date
2024

Document Version
Final published version

Published in
New Challenges in Rock Mechanics and Rock Engineering

Assessment of the influence of discontinuity constitutive models for modelling fractured rock masses

G. Cammarata
Seequent, The Bentley Subsurface Company, Milan, Italy

T.A. Bui & S. Brasile
Seequent, The Bentley Subsurface Company, Delft, The Netherlands

V. Skordilis & R. Brinkgreve
Delft University of Technology, Delft, The Netherlands

ABSTRACT: Understanding and properly simulating discontinuity mechanical behaviour is crucial in all rock engineering projects. Several constitutive relationships have been proposed and implemented in numerical codes. This paper discusses the results of a numerical study that examines the influence of adopting different rock discontinuity constitutive models for simulating the behavior of a fractured rock mass. Two constitutive approaches are employed: an enhanced Coulomb-based criterion with strain softening and a modified version of the Barton-Bandis model to overcome potential implementation issues. These models have been implemented in PLAXIS and their performance is inspected through numerical analyses of an underground cavity for a specific discontinuity network geometry. The results provide insights into the implications and suitability of adopting different discontinuity constitutive models for assessing the stability of engineering works in fractured rock masses.

1 INTRODUCTION

Discontinuities such as joints, bedding planes, and faults govern the mechanical strength and deformation of rock masses. Therefore, thorough knowledge and proper simulation of discontinuity mechanical behaviour have become crucial in all rock engineering projects and nowadays many computational codes allow explicitly modelling discontinuities rather than considering their role within the context of an equivalent continuum representation of the rock mass.

Several theoretical and experimental constitutive models have been proposed (e.g., Patton 1966, Goodman 1976, Barton et al. 1985, Saeb & Amadei 1992, Grasselli & Egger 2003). The accuracy to mimic the discontinuity mechanical response and, in turn, the complexity of these models have increased conjointly with advances in computational methods. Even if the usage of advanced constitutive models to realistically reproduce the discontinuity behaviour is attractive, their strong nonlinearity may provide difficulty for their implementation, with consequent numerical convergence and stability problems (Lei & Barton 2022). In addition, the definition and calibration of the required parameters might be toilsome. A compromise between the complexity (realism) of a constitutive model, the challenge of its numerical implementation, and the definition of its parameters is thus needed. Therefore, conventional models are still more commonly adopted in practical engineering due to their user-friendliness and easy-to-determine parameters.

The purpose of this paper is to numerically assess the influence of using different constitutive laws for modelling discontinuities. The paper initially presents the formulation of two models, along with numerical validation examples: (i) an elasto-plastic constitutive relationship with strain-softening based on Coulomb's failure criterion, and (ii) a constitutive approach aimed at guaranteeing the theoretical rigorousness of the empirically derived formulation of the Barton-

Bandis model for preventing numerical issues. To assess the reliability of the numerical implementation in PLAXIS, the performance of these models is investigated by analyzing the stability of an underground excavation with an imposed discontinuity geometry.

2 CONSTITUTIVE FORMULATIONS

Constitutive models of rock discontinuities are key components for numerical modelling of the physical behavior of fractured rock masses. The development of the models must be able to capture the conceptual behaviour observed in laboratory experiments and/or field observations with a sound mathematical basis. Among the constitutive laws that have been developed, Coulomb's and Barton-Bandis' models have been widely applied in rock engineering analysis and recognized as typical examples of conventional and advanced models, respectively (Skordilis, 2023). The proposed enhancements and modifications to these models are presented hereinafter and the resulting mechanical behaviors are shown in Figure 1.

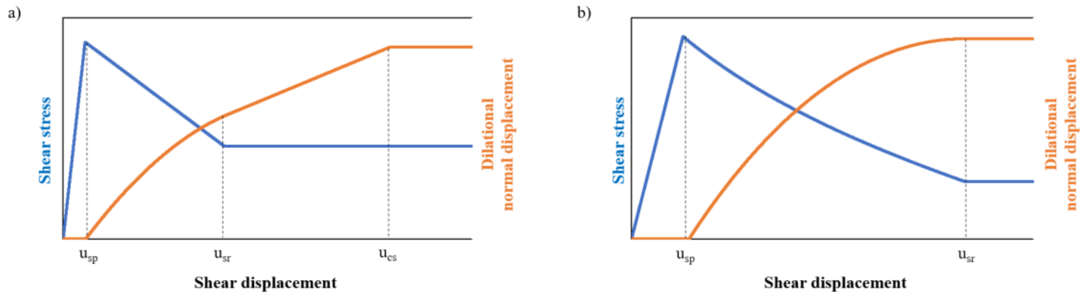

Figure 1. Shear stress-shear displacement and dilational normal displacement caused by shear stress and associated shear displacement for a) Coulomb with softening and b) modified Barton-Bandis models.

The modified formulations deal with the strength and dilation behaviour for ensuring their modelling capabilities and numerical stability. Constant normal and shear stiffnesses are employed.

2.1 *Coulomb with linear softening model*

To represent the discontinuity behaviour, Coulomb's model within a perfect plastic framework has been widely used in numerical analysis. However, such a simple model may only be used if the post-peak drop is negligible (smooth discontinuities and/or high normal stress level).

To make it more generic, the model is thus enhanced according to the constitutive relationship with strain softening proposed by Goodman (1976), which adopts a linear decrease of the post-peak strength with shear displacement (Fig. 1a). This reformulation allows to capture the essential pre- and post-peak characteristics by preserving the ease of use and parameterization of the model. The resulting yield surface is expressed as:

$$F = \tau - (\sigma_n \tan\varphi + c)\left(1 - \frac{\kappa}{Dc}\right) - (\sigma_n \tan\varphi_r + c_r)\left(\frac{\kappa}{Dc}\right) \tag{1}$$

where τ and σ_n are the shear and normal stresses, φ and c are the initial/residual friction angle and cohesion, D_c is the critical slip distance defined as the difference in shear displacement u_s at residual (u_{sr}) and peak (u_{sp}) conditions (i.e., $D_c = u_{sr} - u_{sp}$), and κ is the state parameter representing the accumulated total displacements only during the plastic loading.

Consistently with the mathematical expression of the yield surface in Equation (1), a non-associated plastic flow rule is introduced in the plastic potential with the dilatancy angle ψ:

$$G = \tau - \sigma_n \tan\psi\left(1 - \frac{\kappa}{Dc}\right) - \sigma_n \tan\psi_r\left(\frac{\kappa}{Dc}\right) \tag{2}$$

As depicted in Figure 1a, the shear-induced dilatancy is related to the shear displacements. Dilation occurs at the onset of the plastic sliding and transition to residual conditions happens once the residual shear displacement is reached. The accumulated dilation is limited by a critical shear displacement (u_{cs}) value beyond which the dilation stops (e.g., Min et al. 2004).

2.2 *Modified Barton-Bandis model*

The Barton-Bandis model is a physically motivated empirical model that has been calibrated against extensive experimental measurements and that can properly describe the nonlinear evolution of the pre- and post-peak strength and dilation behaviour. However, due to its strong nonlinearity, the implementation into numerical code can be challenging with consequent numerical convergence and stability issues (Lei & Barton 2022). In addition, its validity ceases for certain stress levels. Mathematical treatments required to overcome these aspects are herein proposed.

In this model, the strength under different normal stress levels is expressed as:

$$\tau = \sigma_n \tan\left(JRC_{mob}\log_{10}\left(\frac{JCS}{\sigma_n}\right) + \varphi_r\right) \tag{3}$$

where JRC_{mob} is the mobilized joint roughness coefficient value related to the amount of shear displacement to its peak value and JCS the joint compressive strength (e.g., Barton et al. 1985). Equation (3) loses its validity for low- and high-stress levels when σ_n approaches zero and JCS, respectively. For low-stress levels, Barton (1976) suggested the criterion envelope is truncated with a steeply inclined linear form and with a maximum allowable friction angle of 70° without any possible cohesion intercept. This is depicted in Figure 2a with the green line inclined at φ_{Tr} equal to 70° and σ_{Tr} identifies the normal stress at the interception with the envelope defined by Equation (3). This approach might be too conservative and would lead to numerical instability. For high-stress levels, there is a lack of experimental evidence, but the mobilized friction angle resulting from Equation (3) decreases to zero and negative values, which is physically incorrect.

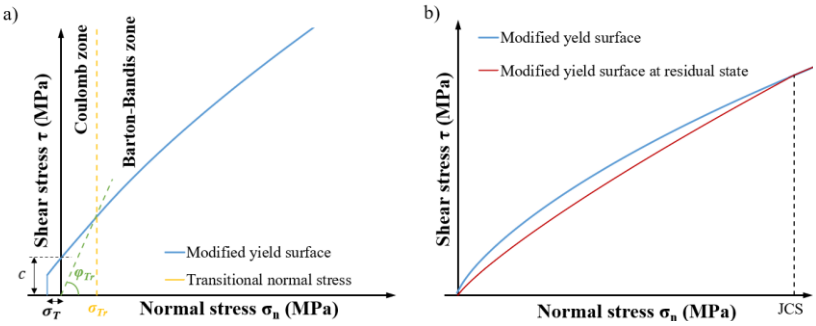

Figure 2. Modified Barton-Bandis model: a) yield surface at low-stress levels;(b) initial/residual envelopes.

Motivated by the mathematical validity and convexity of the yield function (Fig. 2b), the proposed model suggests to smoothly extending the yield surface into $\sigma_n \leq \sigma_{Tr}$ and $\sigma_n \geq$ JCS stress levels with Coulomb envelope sections characterized by equivalent friction angles equal to the tangent slope to the envelope in $\sigma_n = \sigma_{Tr}$ and $\sigma_n =$ JCS, respectively. In addition, a cohesion intercept c, a tensile cut-off σ_t, and a dilatancy angle ψ are introduced, and the same projection is adopted for the residual strength at high stress. Finally, the residual yield surface is the result of a softening process consistent with the approach introduced in Section 2.1. Considering the empirical nature of the highly nonlinear evolution of JRC_{mob}, a linear reduction of JRC_{mob} dictated by the state parameter κ is proposed for the post-peak strength:

$$JRC_{mob} = JRC_{peak}\left(1 - \frac{\kappa}{Dc}\right) \tag{4}$$

This formulation is thus employed for the definition of the yield surface, expressed as follows:

$$F = \tau - \sigma_n \tan\left(JRC_{mob}\log_{10}\left(\frac{JCS}{\sigma_n}\right) + \varphi_r\right) \tag{5}$$

Figure 1b highlights the nonlinear post-peak trend due to the linear reduction of Equation (4).

The following expression for the plastic potential introduces non-associative plasticity:

$$G = \tau - \sigma_n \tan\left(\frac{1}{2}JRC_{mob}\log_{10}\left(\frac{JCS}{\sigma_n}\right)\right) \tag{6}$$

As shown in Figure 1b, no dilation is observed once the residual shear displacement is reached.

3 MODELS VALIDATION

To test the performance of the proposed models, finite element analyses simulating typical laboratory tests have been carried out. For this purpose, the shear tests under constant normal load (CNL) performed by Skinas et al. (1990) are considered. The tests were conducted under loads of 1, 2, and 5 MPa on cast discontinuities from natural surfaces characterized by JRC ranging from 9 to 18, JCS equal to 28 MPa, and pure frictional resistance angle (equivalent to φ_r) of 37°.

Here, the validation concerns only the experimental results obtained with JRC equal to 9. The complete set of calibrated parameters adopted for the numerical analyses is listed in Table 1.

Table 1. Calibrated parameters of Coulomb with softening and modified Barton-Bandis models.

Coulomb with softening		**Modified Barton-Bandis**	
Parameter	Value	Parameter	Value
c	0.342 MPa	JRC	9
c_r	0.270 MPa	JCS	28 MPa
φ	41°	c	0.0035 MPa
φ_r	37°	φ_r	37°
ψ	4°	φ_{Tr}	70°
ψ_r	1.55°	ψ	30°
k_n	25 MPa/mm	k_n	25 MPa/mm
k_s	2.5 MPa/mm	k_s	2.5 MPa/mm
D_c	16 mm	D_c	20 mm
u_{cs}	29 mm	σ_t	0 MPa

The finite element model is shown in Figure 3 and consisted of a single discontinuity between two rigid rock blocks modelled as linear elastic with very high stiffness (Young's modulus *E*=15E3 GPa). Constant normal loads are applied at the top of the upper block and shear displacements of 30 mm are laterally imposed to the lower block.

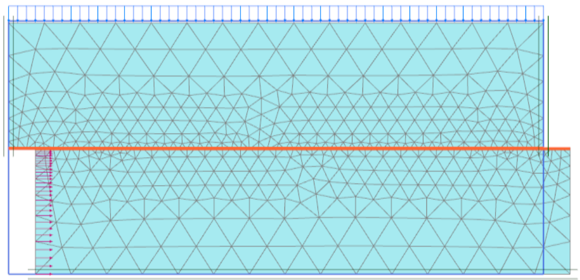

Figure 3. Finite element model for discontinuity shear under CNL conditions.

The results in terms of shear stress versus shear displacement are reported in Figure 4a. Both the implemented models can adequately capture the non-linear behaviour of a discontinuity subjected to shearing under CNL conditions. However, the modified Barton-Bandis model better captures the peak shear strength conditions, while the Coulomb with softening provides a closer approximation of the post-peak behaviour. By using the modified Barton-Bandis model, a slightly conservative prediction of the strength in the post-peak domain is observed. This can be due to the implemented linear softening rule which might imply the residual state is earlier reached.

The discontinuity dilation due to shear is shown in Figure 4b. A close fit is obtained with the Coulomb with softening model, while the modified Barton-Bandis model overpredicts dilation compared to experimental results. Again, this might be due to the implemented softening rule. The same linear reduction of JRC_{mob} applies to both strength and dilation behaviour and, as a consequence, further tuning of the parameters would have also compromised the fitting of the shear stress-displacement curves. This approach was also motivated by considering no experimental data were given for dilation at normal stress values of 2 MPa and 5 MPa.

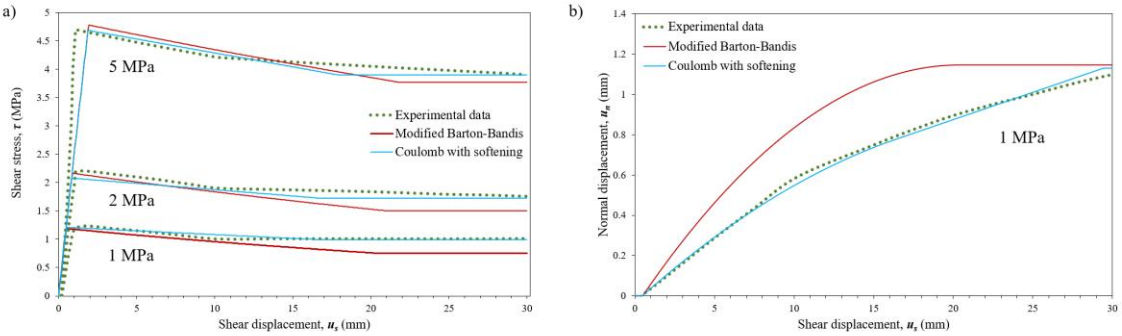

Figure 4. Results of shear CNL tests: (a) shear stress vs. shear displacement, (b) discontinuity dilation.

4 MODELLING AN UNDERGROUND EXCAVATION IN A FRACTURED ROCK MASS

To further investigate the potential of the implemented constitutive laws, the simulation of a circular tunnel, with a diameter of 5.5 m and 800 m deep, in a fractured rock mass is performed (Fig. 5). Being the scope of the analyses to assess the influence of discontinuity laws, a linear elastic and isotropic material is considered for the intact rock blocks with Young's modulus and Poisson's ratio equal to 15 GPa and 0.25, respectively. Two sets of persistent, parallel, and randomly spaced discontinuities characterized by the mechanical properties reported in Table 1 are considered. The plunge of the traces is equal to -55° and 41° for sets 1 and 2, respectively. The spacing is uniformly distributed with a variation between max/min values of 1.0/1.5 m (set 1) and 1.5/2.5 m (set 2). In-situ stress has been defined through the "K_0 procedure", available in PLAXIS, by considering a unit weight of 0.025 MN/m^3 and a K_0 of 0.3. The resulting vertical and horizontal stresses at the tunnel depth are equal to 20 MPa and 6 MPa, respectively.

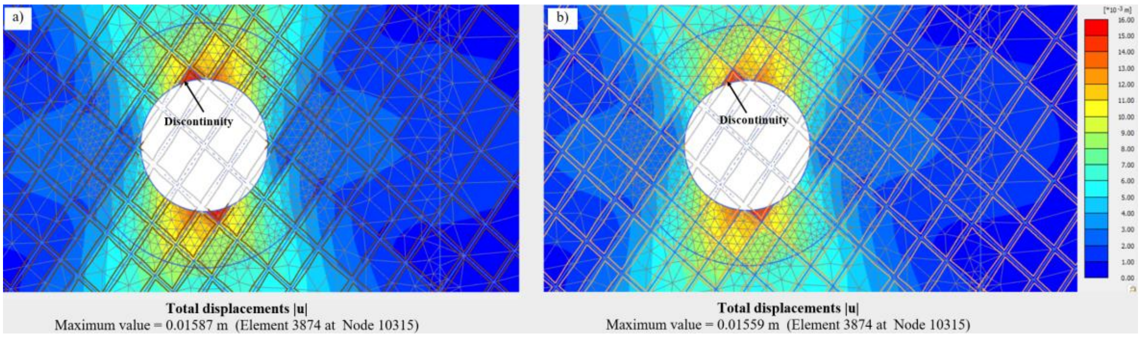

Figure 5. Total displacements: a) modified Barton-Bandis model; b) Coulomb with linear softening.

Figure 5 reports the distribution of displacements around the excavated tunnel. Comparable results are observed by using the two proposed models. In addition, the relatively small values of the displacement imply slight post-peak softening might have occurred without reaching residual states and, in turn, overall stable conditions. However, the analysis of the stresses developed along the discontinuity indicated in Figure 5, which is relative to the most critical wedge, highlights differences between the considered constitutive laws. As shown in Figure 6, the normal stress is negligible closer to the tunnel intersection and increases moving away from the boundary of the excavation. In addition, considerably lower normal and, in turn, shear stress values are obtained with the modified Barton-Bandis model than the Coulomb with softening ones.

These results are explained by considering the discontinuities around the boundary excavations are subjected to low normal stress levels, where differences between the two strength envelopes take place. The Coulomb with softening still allows the mobilization of a significant amount of shear strength due to the cohesion which contributes to the stability of the wedge, while the modified Barton-Bandis has very low shear strength indicating incipient instability of the wedge.

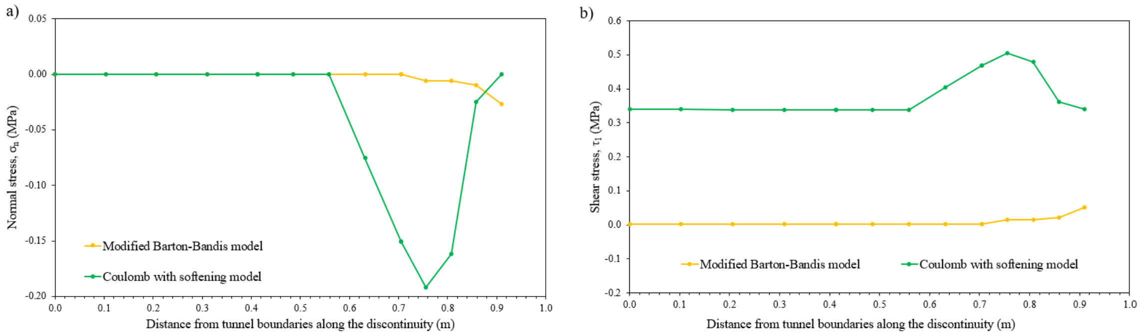

Figure 6. Evolution of a) normal stress and b) shear stress along the discontinuity.

These considerations are confirmed by inspecting the Current relative Stiffness Parameter (CSP) available in PLAXIS, which indicates elastic loading when it is equal to the unity and detection of failure when it approaches zero. At the end of the calculation, CSPs of about 0.01 and 0.2 are inferred for the modified Barton-Bandis and Coulomb with softening models, respectively. These values highlight the capability of the modified Barton-Bandis to detect instabilities.

5 CONCLUSIONS

The formulation of two constitutive relationships for discontinuities implemented in PLAXIS has been described and their reliability has been proven through the validation against laboratory test results. The effect of using these discontinuity models on the stability of fractured rock masses has been examined by carrying out a numerical study of a deep underground excavation with an imposed discontinuity geometry. The results in terms of deformations indicated that the investigated constitutive laws predict comparable results. The detailed evaluation of potential instabilities has shown that at low-stress levels the modified Barton-Bandis model provides a more conservative solution than the Coulomb with softening model for the analyzed engineering problem.

To better constrain the implications and suitability of adopting different constitutive models, rock engineering practitioners should first consider the stress ranges to which the engineering work to be designed is subjected. Engineering judgment is required to evaluate how to efficiently model discontinuities based on the effectiveness of the model and its parameters calibration.

REFERENCES

Barton, N. 1976. The shear strength of rock and rock joints. *Int J Rock Mech Min Sci & Geomech Abstr*, 13 (9): 255–279.

Barton, N., Bandis, S. & Bakhtar, K. 1985. Strength, deformation and conductivity coupling of rock joints. *Int J Rock Mech Min Sci & Geomech Abstr*, 22 (3): 121–140.

Goodman, R.E. 1976. *Methods of geological engineering in discontinuous rocks*. St Paul: West Publ. Co.

Grasselli, G. & Egger, P. 2003. Constitutive law for the shear strength of rock joints based on three-dimensional surface parameters. *Int J Rock Mech Min Sci*, 40 (1): 25–40.

Lei, Q. & Barton, N. 2022. On the selection of joint constitutive models for geomechanics simulation of fractured rocks. *Computers and Geotechnics*, 145: 104707.

Min, K.-B., Rutqvist, J., Tsang, C.-F., Jing, L., 2004. Stress-dependent permeability of fractured rock masses: a numerical study. *Int J Rock Mech Min Sci* 41 (7): 1191–1210.

Skinas, C., Bandis, S. & Demiris, C. 1990. Experimental investigations and modelling of rock joint behaviour under constant stiffness. *Proc. Int. Symp. on Rock Joints, Loen, Norway*, Balkema, 301–308.

Skordilis, V. 2023. Finite element analysis of fractured rock mass with PLAXIS 2D using different discontinuity constitutive models. MSc thesis, Delft University of Technology, Delft, The Netherlands.

Patton, F.D. 1966. *Multiple modes of shear failure in rock and related materials*. PhD thesis, Uni of Illinois.

Saeb, S. & Amadei, B. 1992. Modelling rock joints under shear and normal loading. *Int J Rock Mech Min Sci & Geomech Abstr*, 29(3): 267–278.